

Supporting Information

Bimodal nanolatexes prepared via polymerization-induced self-assembly: losing control in a controlled manner

Alexandros E. Alexakis^{a,b}, Olivia R. Wilson^a and Eva Malmström^{a,b*}

^a KTH Royal Institute of Technology, School of Engineering Sciences in Chemistry, Biotechnology and Health, Department of Fibre and Polymer Technology, Division of Coating Technology, Teknikringen 56-58, SE-100 44 Stockholm, Sweden.

^b Wallenberg Wood Science Centre (WWSC), Teknikringen 56-58, SE-100 44 Stockholm, Sweden.

* Corresponding authors e-mail: mavem@kth.se

Table of Contents

1. THF-SEC of the CCCPA RAFT-agent	2
2. RAFT polymerization of PDMAEMA – synthesis of macroRAFT agents.....	3
3. RAFT-mediated PISA of MMA – synthesis of nanolatexes	4
4. Molecular weight and dry content calculation	4
5. ¹ H-NMR spectra of macroRAFT agents.....	5
6. Properties of macroRAFT agents	6
7. THF-SEC and DSC results of bimodal nanolatexes.....	6
8. Reproducibility studies	10
9. FE-SEM of THFMA nanolatexes.....	11
10. QCM-D results of the bimodal nanolatexes.....	12
11. Drying experiments	14

1. THF-SEC of the CCCPA RAFT-agent

The chromatogram of the CCCPA RAFT agent is shown in Figure S1.

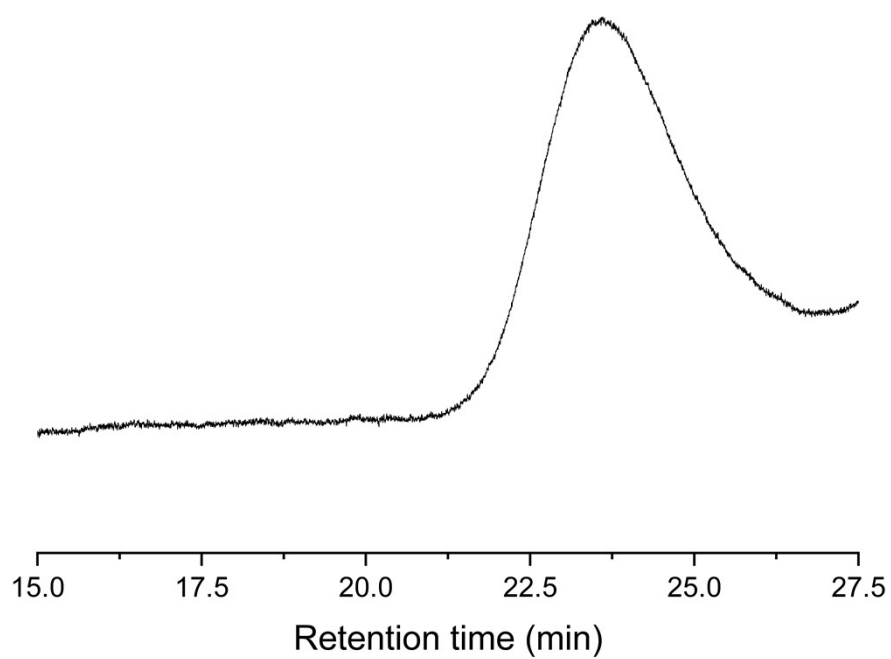


Figure S1 – Normalized RI signal of the CCCPA RAFT-agent by THF-SEC.

2. RAFT polymerization of PDMAEMA – synthesis of macroRAFT agents

All amounts used to synthesize macroRAFT agents can be found in Table S1.

Table S1 - Analytical values of reagents used for the RAFT polymerization of DMAEMA in water.

Samples	DMAEMA (mL, mmol)	CCCPA (g, mmol)	AIBA (mL, mmol) ^a	H ₂ O (mL) ^b
D ₇	1.56, 9.4	0.41, 1.35	12.9, 0.16	16.95
D ₂₅	2.03, 12.2	0.15, 0.49	4.7, 0.06	18.67

^a Volume of AIBA from a stock solution of 3.4 g/L in deionized water. ^b Volume of deionized water calculated from equation S2 in order to have a dry content of 10 wt%.

Additionally, the livingness of the polymer chains was calculated based on equation S1:

$$L = \frac{[RAFT]_o}{\left([RAFT]_o + \left(2 \cdot f \cdot [I]_o \cdot (1 - e^{-k_d t}) \cdot \left(1 - \frac{f_c}{2}\right)\right)\right)}$$

(S1)

where $[RAFT]_o$ is the initial concentration of RAFT agent, $[I]_o$ is the initial concentration of the initiator, f_c is the coupling factor (termination by disproportionation was assumed for PDMAEMA, $f_c=0$).

$2 \cdot f \cdot [I]_o \cdot (1 - e^{-k_d t})$ refers to the total number of radicals generated from the initiator over the polymerization time, where f is the initiator efficiency (assumed to be 0.6) and k_d is the decomposition rate constant for AIBA (half-life ($t_{1/2}$) is 100 min at 70 °C in water, hence $k_d = \frac{\ln 2}{t_{1/2}} = 1.16 \cdot 10^{-4} \text{ sec}^{-1}$).

For D₇ and D₂₅, L is 93 and 97 %, respectively.

3. RAFT-mediated PISA of MMA – synthesis of nanolatexes

The analytical values of each reagent used for the preparation of PISA nanolatexes are listed in Table S2.

Table S2 - Analytical values of reagents used for the RAFT-mediated polymerization-induced self-assembly of MMA and THFMA in water.

Samples	MMA/THFMA (mL, mmol)	macroRAFT (g, mmol)	AIBA (mL, μmol) ^a	H ₂ O (mL) ^b
D ₇ -M ₂₀₀	2.13, 20.0	0.15, 0.10	0.97, 12.0	19.44
D ₇ -M ₅₀₀	2.22, 20.9	0.06, 0.04	0.40, 5.1	19.45
D ₂₅ -M ₃₈₀	2.03, 19.0	0.21, 0.05	0.48, 6.1	19.06
D ₂₅ -M ₅₀₀	2.10, 19.6	0.17, 0.04	0.38, 4.7	19.20
D ₂₅ -T ₁₀₀	0.48, 2.9	0.13, 0.03	0.28, 4.0	5.35
D ₂₅ -T ₂₀₀	0.54, 3.3	0.07, 0.02	0.16, 2.0	5.53
D ₂₅ -T ₃₀₀	0.54, 3.3	0.05, 0.01	0.11, 1.0	5.37

^a Volume of AIBA is from a stock solution of 3.4 g/L in deionized water. ^b Volume of deionized water is calculated from equation S4 in order to have a dry content of 10 wt%.

4. Molecular weight and dry content calculation

The theoretical molecular weight (M_n) of the macroRAFT agents was calculated by using equation S3 based on the degree of polymerization (DP) obtained by their respective ¹H-NMR spectra.

$$DP = \frac{I_{PDMAEMA \text{ polymer peak}}}{I_{RAFT \text{ agent peak}}} = \frac{I_{3.5 \text{ ppm}}}{I_{2.5 \text{ ppm}}} \quad (\text{S2})$$

$$M_n = (DP \cdot M_{DMAEMA}) + M_{RAFT} \quad (\text{S3})$$

Where M_{DMAEMA} is the molecular weight of DMAEMA (157.21 g/mol) and M_{RAFT} is the molecular weight of the CCCPA RAFT agent (307.41 g/mol).

Equation S4 is used for the calculation of the theoretical dry content ($\tau_{theor.}$) assuming a 100% conversion of monomer to polymer.

$$\tau_{theor.} (\%) = \left[\frac{(m_{macroRAFT}^{initial} + m_{monomer}^{initial})}{(m_{macroRAFT}^{initial} + m_{monomer}^{initial} + m_{H_2O})} \right] \cdot 100$$

(S4)

Where $m_{macroRAFT}^{initial}$ is the initial mass of macroRAFT (g), $m_{monomer}^{initial}$ is the initial mass of MMA or THFMA (g) and m_{H_2O} is the mass of water (g).

5. ¹H-NMR spectra of macroRAFT agents

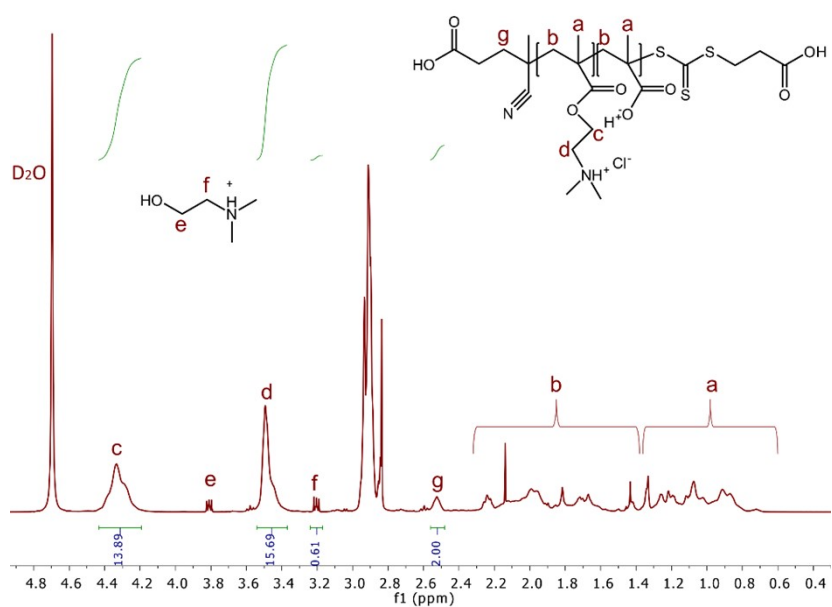


Figure S2 - ¹H-NMR of macroRAFT D₇ in D₂O.

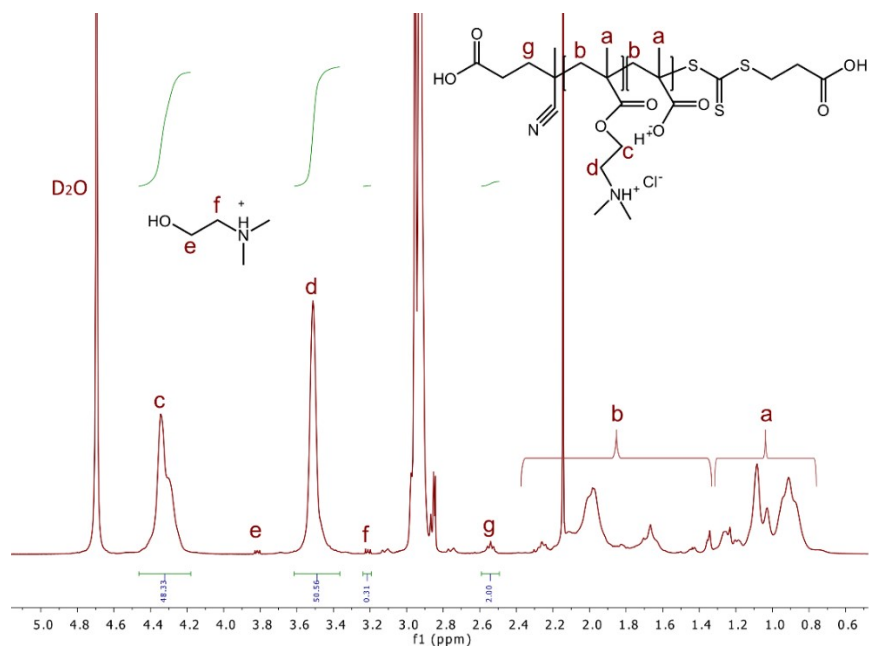


Figure S3 - $^1\text{H-NMR}$ of macroRAFT D_{25} in D_2O .

The conversion (p) of the RAFT polymerization of DMAEMA in water was evaluated by $^1\text{H-NMR}$ in D_2O at different time intervals. The conversion was calculated by using equation S5, where the double bonds of DMAEMA noted with (a) are correlated to the resulting broad polymer peak noted with (b).

$$p (\%) = \left[\frac{\left(\frac{I_{0.8-1.2 \text{ ppm}}}{3} \right)}{\left(\left(\frac{I_{5.7 \text{ ppm}} + I_{6.1 \text{ ppm}}}{2} \right) + \left(\frac{I_{0.8-1.2 \text{ ppm}}}{3} \right) \right)} \right] \cdot 100 = \left[\frac{\left(\frac{b}{3} \right)}{\left(\left(\frac{a+a}{2} \right) + \left(\frac{b}{3} \right) \right)} \right] \cdot 100$$

(S5)

6. Properties of macroRAFT agents

The physicochemical properties of the macroRAFT agents are listed in Table S3.

Table S3 - Physicochemical properties of the macroRAFT agents.

Samples	p (%) ^a	DH (%) ^b	M_n (g/mol) ^c	Charge Density ($\mu\text{mol/g}$) ^d	T_g ($^{\circ}\text{C}$) ^e
D₇	88	3.7	1540	996 ± 13	75.1 ± 3.9
D₂₅	99	0.6	4220	3095 ± 50	120.0 ± 1.5

^a Monomer conversion calculated by equation S5. ^b Degree of hydrolysis occurring during the RAFT polymerization of DMAEMA in water calculated according to ref. ^c Theoretical molecular weight calculated by equation S3. ^d Obtained from PET. ^e Obtained from the second heating cycle of DSC.

7. THF-SEC and DSC results of bimodal nanolatexes

The normalized THF-SEC data for the nanolatexes based on the RI detector are plotted against retention time in Figure S4.

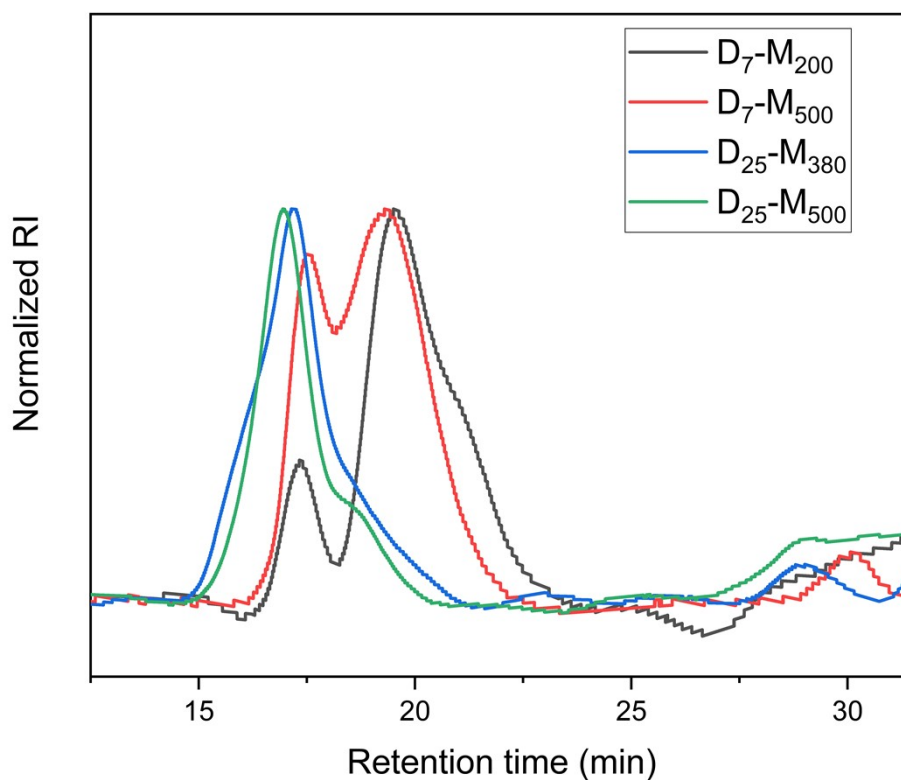


Figure S4 – THF-SEC data of the bimodal nanolatexes based on RI detector and PS calibration standards.

The molecular weight and polydispersity (\mathcal{D}) of the bimodal nanolatexes is listed in Table S4.

Table S4 – Theoretical and experimental molecular weight for the nanolatexes.

Samples	M_n	M_n (\mathcal{D})
	(g/mol) ^a	10^6 (g/mol) ^b
D₇-M₂₀₀	18700	0.7 and 0.1 (1.58)
D₇-M₅₀₀	45100	0.6 (1.58)
D₂₅-M₃₈₀	36600	1.1 and 0.7 (1.58)
D₂₅-M₅₀₀	46800	1.1 (1.58)

^a Molecular weight calculated from equation S3. ^b Number average molecular weight and polydispersity obtained from THF-SEC with PS standards. The values listed are from the IR-detector.

In a case study the D₂₅-M₅₀₀ lyophilized sample was dissolved in THF-*d*₈ and the ¹H-NMR spectra was recorded in Figure S5 where characteristic polymer peaks can be seen.

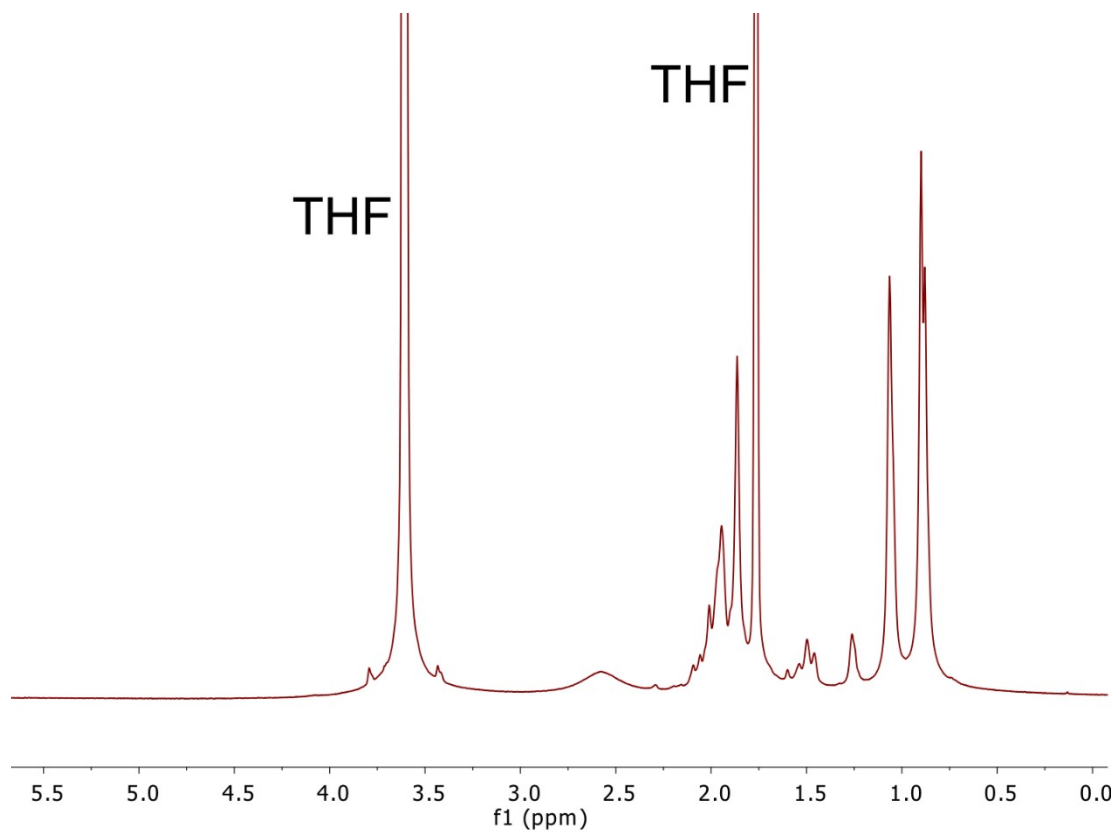


Figure S5 – ¹H-NMR of D₂₅-M₅₀₀ in THF-*d*₈.

Aliquots from the polymerization of D₂₅-M₅₀₀ were also analysed by THF-SEC and plotted against retention time in Figure S6.

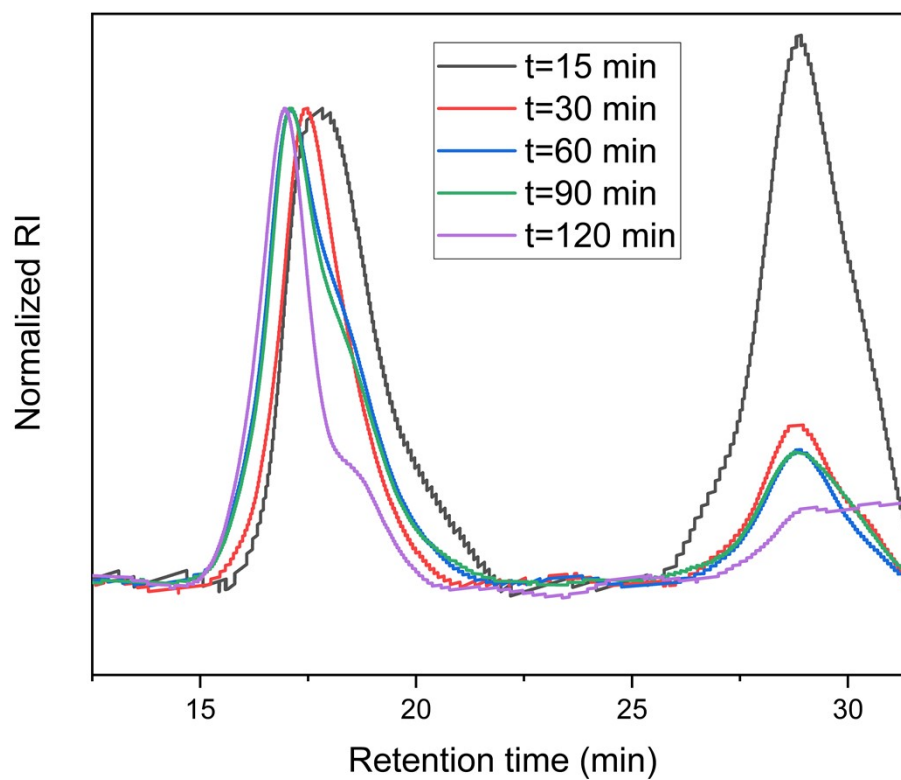


Figure S6 – THF-SEC data of the D_{25} - M_{500} based on RI detector and PS calibration standards.

The DSC curves of the bimodal nanolatexes are shown in Figure S7.

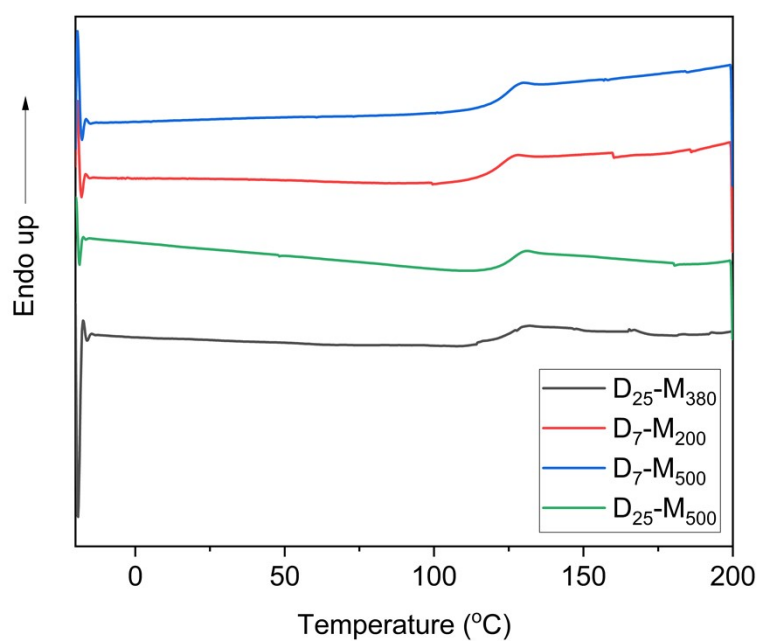


Figure S7 – DSC curves of the bimodal nanolatexes.

8. Reproducibility studies

The batch reproducibility of the bimodality was studied for D₂₅-M₃₈₀ and D₂₅-M₅₀₀ by DLS and FE-SEM. The data listed in Table S5 show the D_H , D_{large} , D_{small} and PdI for the nanolatexes and in Figure S8, the bimodal morphology of D₂₅-M₃₈₀ is shown as an example. The batch reproducibility could not be verified for the D₇ containing nanolatexes due to lack of material.

Table S5 - Batch reproducibility based on DLS and FE-SEM.

Sample Name	Batch	P (%) ^a	D_H (nm) ^b	PdI ^b	D_{large} (nm) ^c	D_{small} (nm) ^c
D ₂₅ -M ₃₈₀	1	75	133 ± 2	0.02 ± 0.01	90 ± 11	37 ± 9
	2	85	112 ± 2	0.04 ± 0.01	78 ± 5	32 ± 4
	3	86	100 ± 3	0.03 ± 0.01	65 ± 4	31 ± 5
D ₂₅ -M ₅₀₀	1	85	120 ± 1	0.03 ± 0.01	---*	---*
	2	80	136 ± 2	0.03 ± 0.01	125 ± 12	62 ± 9
	3	75	143 ± 4	0.03 ± 0.01	117 ± 11	47 ± 7

^a MMA conversion determined gravimetrically using equation S4. ^b Obtained from DLS at 0.1 wt% in deionized water. ^c Diameter of small (D_{small}) and large (D_{large}) nanolatexes measured by FE-SEM on spin-coated silica at 0.1 wt% were evaluated with the Gwyddion software. * FE-SEM analysis was not performed.

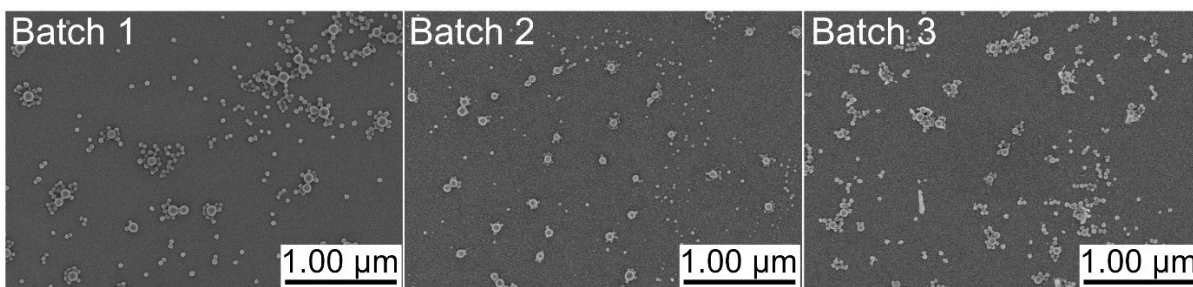


Figure S8 – FE-SEM of D_{25} - M_{380} for three batches. The scale bar in all images is 1 μm .

9. FE-SEM of THFMA nanolatexes

Cationically charged nanolatexes with D25 were synthesized by using THFMA of DP 100, 200, and 300, referred to as T_{100} , T_{200} , and T_{300} , respectively, and they were spin-coated on silica and imaged by FE-SEM (Figure S9).

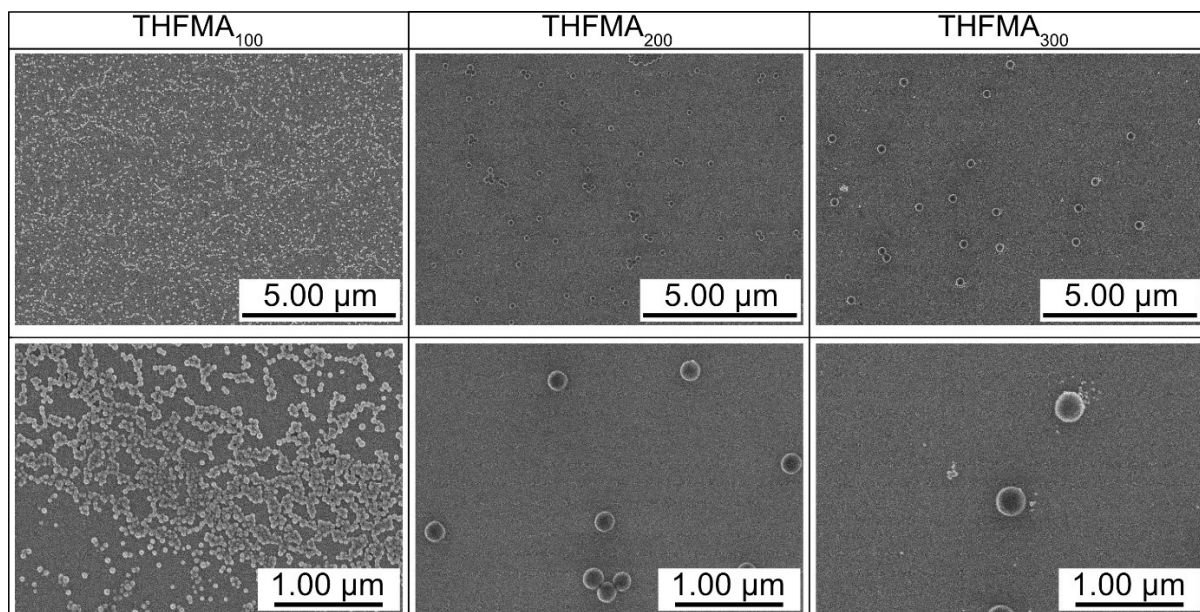


Figure S9 – FE-SEM of $D_{25}\text{-}T_{100}$, $D_{25}\text{-}T_{200}$ and $D_{25}\text{-}T_{300}$. The scale bar on the top images is 5 μm and the bottom 1 μm.

10. QCM-D results of the bimodal nanolatexes

The dissipation of the adsorption of nanolatexes is shown in Figure S10.

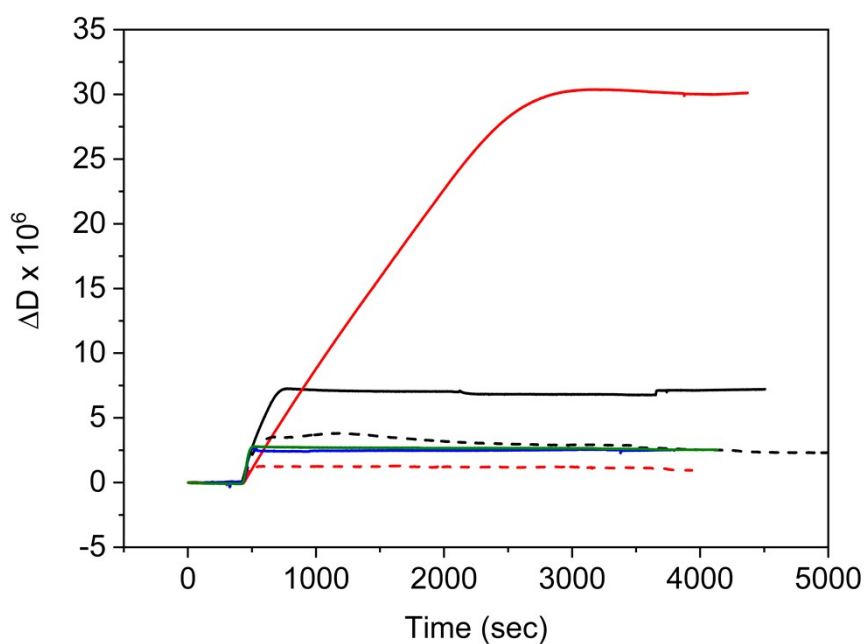


Figure S10 – Dissipation of nanolatexes; Monomodal nanolatexes: D_7-M_{100} (black dashed line) and $D_{25}-M_{200}$ (red dashed line) and bimodal nanolatexes: D_7-M_{200} (black line), D_7-M_{500} (red line), $D_{25}-M_{380}$ (blue line) and $D_{25}-M_{500}$ (green line).

Table S6 – QCM-D results for the mono- and bimodal nanolatexes.

Sample Name	Size Distribution ^a	Δf (Hz)	Γ (mg/m ²)	ΔD $\times 10^6$
D_7-M_{100}	M	-106.4 ± 0.9	6.28 ± 0.04	2.9 ± 0.1
D_7-M_{200}	B	-110.0 ± 4.2	6.5 ± 0.1	7.0 ± 0.3
D_7-M_{500}	B	-238.0 ± 24.0	14.1 ± 0.7	31.9 ± 2.6
$D_{25}-M_{200}$	M	-25.4 ± 2.4	1.5 ± 0.1	0.9 ± 0.3
$D_{25}-M_{380}$	B	-22.0 ± 9.0	1.3 ± 0.3	2.2 ± 0.5
$D_{25}-M_{500}$	B	-29.4 ± 8.4	1.7 ± 0.3	1.7 ± 1.3

^a monomodal (M) and bimodal (B) nanolatexes.

After monitoring their adsorption with QCM-D, the substrates were imaged by FE-SEM (Figure S11).

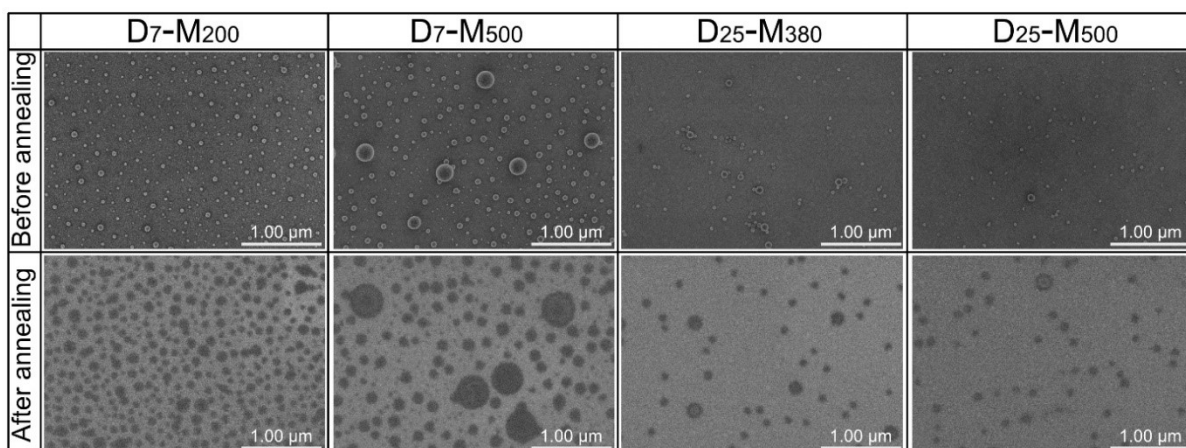


Figure S11 – FE-SEM of nanolatex-adsorbed QCM-D substrates before (top) and after (bottom) annealing at 150 °C for 5 h. The scale bar in all images is 1 μm.

The contact angle against water of the nanolatex-adsorbed QCM-D substrates is shown in Figure S12.

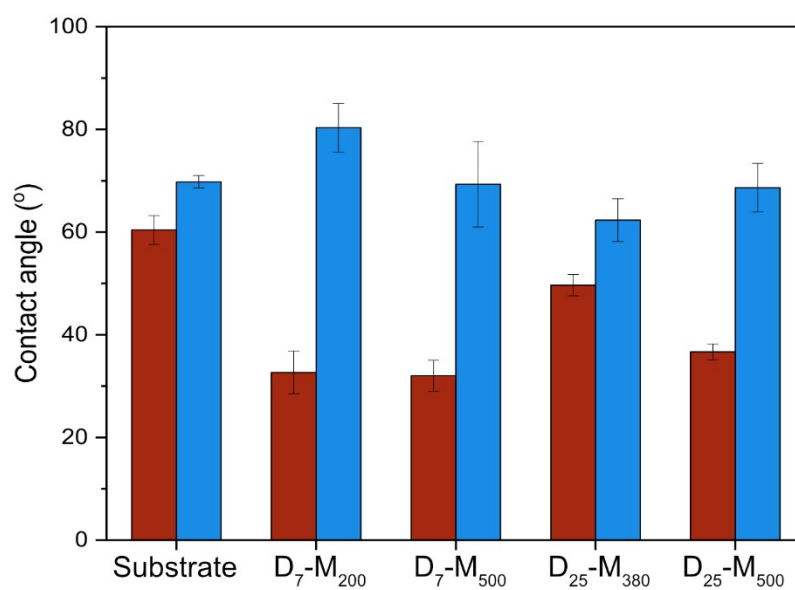


Figure S12 – Contact angle against water of the QCM-D substrates before (red) and after (blue) annealing at 150 °C for 5 h.

11. Drying experiments

The contact angle against water of the annealed nanolatex-modified filter papers is plotted in Figure S13. The values for the same samples before annealing were 0 and are not presented in the Figure S13.

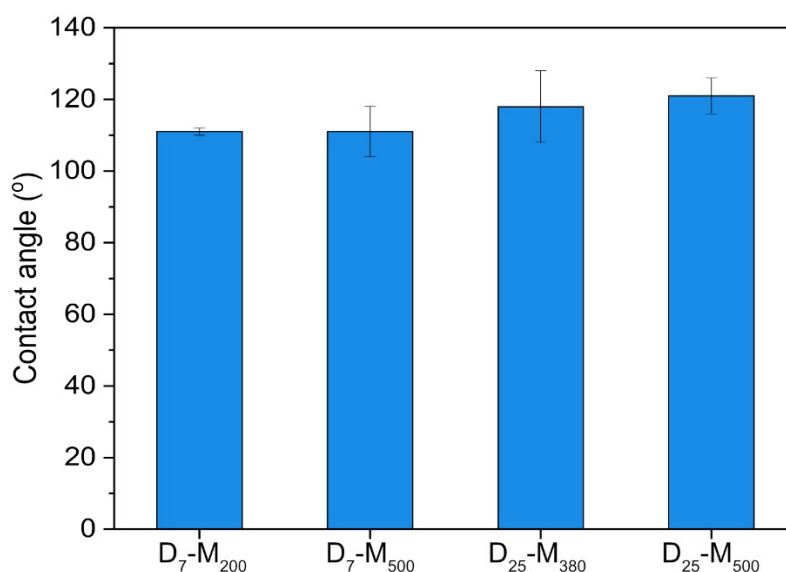


Figure S13 – Contact angle against water of the nanolatex-modified filter papers after annealing at 150 °C for 5 h.

Additionally, silica wafers modified with 0.025 g/L of nanolatex dispersions and dried in the conditioning room or in an oven at 150 °C for 3 min were imaged by FE-SEM (Figure S14).

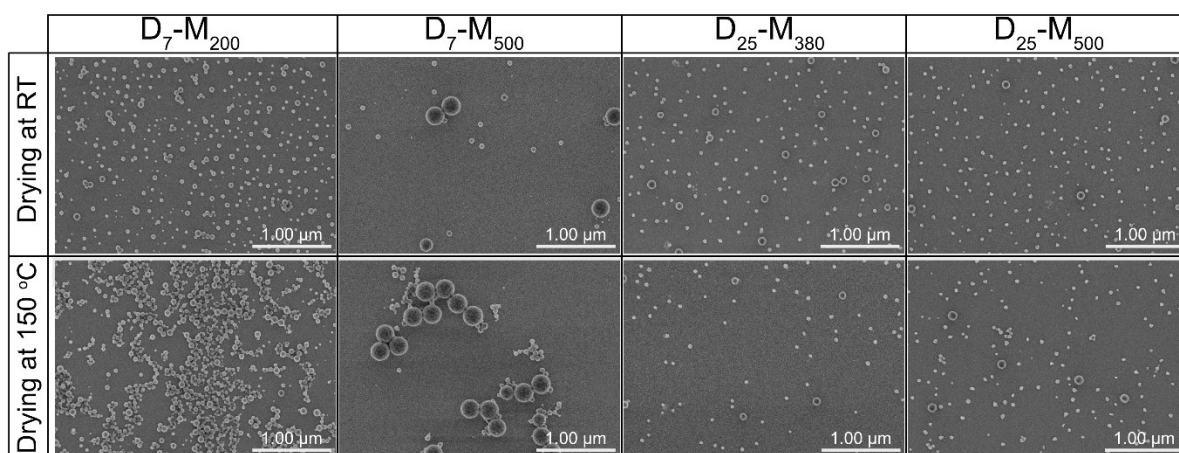


Figure S14 – FE-SEM of silica wafers modified with nanolatexes; Dried in the conditioning room (top) and in an oven at 150 °C for 3 min (bottom). The scale bar in all images is 1 μm.

The contact angle against water of the silica wafers after they were dried in the conditioning room or in an oven at 150 °C for 3 min was plotted in Figure S15.

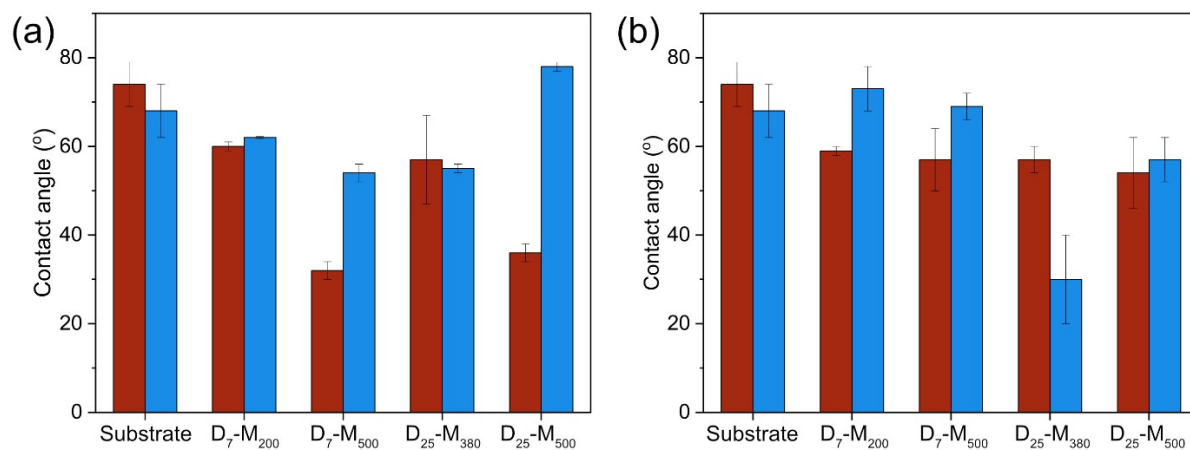


Figure S15 – Contact angle against water of the nanolatex-modified silica wafers when dried in the conditioning room (red) and in an oven at 150 °C for 3 min (blue) at 0.025 g/L (a) or 0.1 wt% (b).